

Thermal force effects on slowly rotating, spherical artificial satellites—I. Solar heating

Paolo Farinella¹ and David Vokrouhlický²

¹Gruppo di Meccanica Spaziale, Dipartimento di Matematica, Università di Pisa, Via Buonarroti 2, 56127 Pisa, Italy

²Institute of Astronomy, Charles University, Švédská 8, 15000 Prague 5, Czech Republic

Received 12 January 1996; revised 24 April 1996; accepted 24 April 1996

Abstract. The heating of a spinning artificial satellite by natural radiation sources such as the Sun and the Earth results in temperature gradients arising across the satellite's surface. The corresponding anisotropic emission of thermal radiation leads to a recoil force, commonly referred to as "thermal force". A quantitative theory of this effect is developed, based on more general assumptions than used so far, to model such radiation forces on spherically symmetric LAGEOS-like satellites. In particular, the theory holds for any ratio of the three basic timescales of the problem: the rotation period of the satellite, the orbital period around the Earth, and the relaxation time for the thermal processes. Thus, the simplifying assumption of a comparatively fast rotational motion is avoided, which will fail for LAGEOS within the next decade, owing to magnetic dissipation effects. A number of predictions about the future behaviour of non-gravitational long-term orbital perturbations of LAGEOS become possible with the new theory. In particular the Yarkovsky-Schach thermal force effects are studied arising as a consequence of the solar radiation flux onto the satellite, periodically interrupted by eclipses. Starting on about year 2005, the orbital perturbation effects predicted by the new theory are substantially different from those inferred in the fast-rotation case. This holds not only for the long-term semimajor axis effects, but also for eccentricity and inclination perturbations. Copyright © 1996 Elsevier Science Ltd

1. Introduction

The passive artificial satellite LAGEOS is the celestial body with the most precisely known orbit. Current laser

tracking technology allows an accuracy of the order of 1 cm in determining its position, with the available data spanning about two decades. As a result, LAGEOS orbit analysis has led to valuable information on a number of geophysical processes, such as Earth rotation, geopotential harmonics and their time variations, tectonic plate motions, and tides to be derived. At the same time, the tracking data have shown that dynamical models aimed at reconstructing/predicting the long-term evolution of LAGEOS's orbital elements (or better, of their time derivatives, or *excitations*) should include a number of tiny non-gravitational forces, related to the interaction of the satellite with the radiation and particle flux present in space. The study of these dynamical effects has presented a number of complex problems, at the borderline between celestial mechanics and environmental physics.

The most precisely determined orbital element is the semimajor axis a . Its changes ($\approx 1 \text{ mm day}^{-1}$ for LAGEOS, over a value of about 12,270 km) can be translated into a time series for the along-track component of the perturbing force acting on the satellite. The data clearly show a secular decrease of a , corresponding to an average drag-like perturbing acceleration of $-3.4 \times 10^{-12} \text{ m s}^{-2}$, which must have a non-gravitational origin. This secular effect is modulated by long-periodic oscillations, for which a number of both gravitational and non-gravitational mechanisms have been suggested (Rubincam, 1982; Barlier *et al.*, 1986; Milani *et al.*, 1987; Scharroo *et al.*, 1991).

Rubincam (1987, 1988, 1990) proposed that the dominant role in generating the secular part of this perturbation is played by "thermal thrust" (or "drag") effects—a recoil force due to thermal radiation anisotropically emitted from the satellite's surface, which is differentially heated by external radiation sources. Due to the relatively fast rotation of LAGEOS, the temperature was considered as constant along any "parallel" on the satellite's surface, and only latitude-dependent temperature changes were seen as relevant—giving rise to a "seasonal" variant of

the classical Yarkovsky thermal effect known in solar system dynamics for a long time (for a review, see Burns *et al.* (1979)). According to Rubincam's analysis, up to 70% of the secular semimajor axis decay and a significant portion ($\approx 50\%$) of the long-term oscillations are caused by this thermal effect, with the infrared radiation flux coming from the Earth as the source of differential heating of the satellite surface (hereinafter this will be referred to as the *Yarkovsky–Rubincam effect*). Soon afterwards, it was realized that the eclipse-related spikes apparent in the semimajor axis residuals may also be explained by a similar effect, triggered by the eclipse-modulated visible sunlight flux (hereinafter this will be called the *Yarkovsky–Schach effect*; see Slabinski, 1988; Afonso *et al.*, 1989; Scharroo *et al.*, 1991). Other likely contributors to the observed semimajor axis residuals include neutral and charged particle drag, Earth-albedo radiation pressure, solar radiation pressure at the Earth's penumbra crossings, and a possible anisotropy in the optical properties of the satellite's surface.

At the beginning of the 1990s, it became clear that a further complicating factor should be taken into account if the dynamical models are aimed at a quantitative match of the orbital data, including not only the semimajor axis but also the eccentricity/perigee excitations (see, e.g. Tapley *et al.*, 1993). Since thermal effects depend sensitively on the orientation of the spin axis and since this direction is not directly observed, one can either derive it from a dynamical model, or solve for it while fitting the along-track orbit residuals. Rubincam applied the latter, inverse method in analysing the LAGEOS data. First, he assumed a constant orientation of the LAGEOS axis, with the best-fitting solution corresponding well to the in-orbit injection data reported by the flight control centre at launch time. Later on, however, it was realized that the spin axis direction could not have remained the same since the time of launch. This was suggested by the unavoidable presence of disturbing torques, and also by the deficiencies of the constant-orientation model in reproducing the observed semimajor axis residuals. To derive the evolution in time of the spin axis direction, two approaches were again tried: (i) an empirical one, determining from the orbital data a set of best-fitting spin axis directions over a sequence of relatively short intervals of time, and fitting these successive positions with a regular curve (Ries *et al.*, 1993; Robbins *et al.*, 1994); (ii) a theoretical one, based on a dynamical model for the torques which affect the rotation of the satellite (Bertotti and Iess, 1991). In the former approach, like in the original Rubincam work, there is no way to distinguish between the two senses of rotation about a given axis in space. This implicitly led a number of authors not to distinguish between the two corresponding sets of initial conditions, both of which were consistent with in-orbit injection data.

However, the situation is different when the evolution of LAGEOS's rotation is derived from a dynamical model, such as that developed by Bertotti and Iess. The differential equations derived by these authors for the components of the satellite's rotation rate vector are *not* invariant with respect to a change in the sense of rotation, and therefore it is essential to choose initial conditions corresponding to the correct sense of rotation. This has

been recently shown by Farinella *et al.* (1996), who have derived a satisfactory, self-consistent solution for the coupled evolution of LAGEOS's spin axis and along-track orbit residuals. Using the same model for the spin axis evolution, Métris *et al.* (1996) have also tackled the problem of adjusting the dynamical parameters to fit the eccentricity/perigee excitations as well, and have come to the surprising conclusion that this is possible only provided the value for the amplitude of the Yarkovsky–Schach effect is about 1.75 times greater than was expected from the previous thermal models of the satellite. This is one of the reasons which have prompted us to reanalyse the problem of how the thermal effects are modelled, and thus have led to this paper.

Actually, there are several issues which appear worth further study. First, the original thermal models assumed a homogeneous satellite body, or anyway an unrealistically simple structure for it. On the other hand, it has been recently shown by Slabinski (1996) that the real complex structure of the satellite results in the fact that its individual components (the retroreflectors, their ring mountings, the metallic interior) have different responses and sensitivities to the visible and infrared heating. In other words, their individual thermal histories are significantly different from the average ones inferred from the ideal homogeneous case. Slabinski's work is a clear step forward in modelling these subtle effects, yet the theory still needs empirical corrections when applied to the observed orbital data.

Second, all the previous analyses did not include the Earth-reflected sunlight as a heating source affecting the temperature distribution across the satellite surface. Métris and Vokrouhlický (1996) recently determined the main effects of this additional radiation source. They concluded that the only significant perturbation, within the current accuracy of the tracking data, is a small additional drag-like acceleration, with a constant value $\approx -0.3 \text{ pm s}^{-2}$.

Third and most relevant here, all the previous thermal force models adopted the simplifying approximation of a fast rotation of the satellite, such that only the "seasonal" (latitude-dependent) component of the temperature gradient is significant and therefore the perturbing force is always directed along the spin axis. Here "fast rotation" means that the spin period is much shorter than the thermal relaxation timescale of the satellite structure. This was a suitable assumption in the early years of the LAGEOS mission (as the initial rotation period was less than 1 s, compared to about 1 h for the thermal relaxation time). However, according to the Bertotti and Iess theory and the Farinella *et al.* solution mentioned above, LAGEOS's rotation rate is decreasing exponentially with time under the action of magnetic torques, and in about 10 years the spin period will reach a value of 3000 s, comparable to the thermal lag time. As a consequence, a more complex thermal and dynamical model will then be required, with the resulting force depending also on the sense of rotation.

Therefore, we have decided to develop a more general theory for the thermal effects acting on the LAGEOS satellite, which removes the fast rotation assumption. In other words, we shall not impose any a priori constraint on the ratio between the satellite rotation period and the

thermal lag time, but allow for any value of this parameter. In this situation, “diurnal” (i.e. longitudinal) temperature gradients on the satellite surface will no longer be negligible, and the net thermal force will tilt from the direction of the spin axis. The corresponding “equatorial” components of the thermal force are those which appear in the classical formulation of the Yarkovsky effect (see, e.g. Peterson, 1976; Burns *et al.*, 1979). Note that because the thermal lag time is comparable to the revolution period of LAGEOS around the Earth, we will also have to allow for a wide range of values of the parameter $r \equiv T_{\text{orb}}/T_{\text{rot}}$, namely the ratio of the satellite’s revolution period T_{orb} to its rotation period T_{rot} . The only limitation of our theory is that it will not be applicable for r close to or smaller than unity, because the spin axis evolution of Farinella *et al.* (1996), which we are going to use, has been obtained by integration of the averaged Euler equations, which fails at the 1:1 ($r = 1$) spin-orbit resonance (see Habib *et al.*, 1994).

In this paper, we will develop a general theory for the satellite thermal response to the external heating sources, and then apply it to the specific case when the heating source is the Sun. In other words, we are going to generalize the previous treatments of the Yarkovsky–Schach effect. A forthcoming paper will be devoted to a similar general treatment of the Yarkovsky–Rubincam effect, with the Earth IR radiation as the heating source.

Before proceeding to the mathematical formulation of the problem, it is worth stressing a few general concepts. There are three natural timescales entering our analysis: (i) the satellite rotation period T_{rot} , (ii) the satellite revolution period T_{orb} , and (iii) the thermal relaxation time τ_R . An even more general formulation would need to account also for the timescale characterizing the evolution of the spin axis direction and of the direction of the radiation source (the Sun in this paper). In our particular problem the latter timescales are much longer (one year or more) than the previously mentioned ones, hence we can consider fixed orientations of the satellite spin axis and of the heating source over the longest time among $(T_{\text{rot}}, T_{\text{orb}}, \tau_R)$.

Our goal is to derive expressions for the long-term orbital effects, that is for the averaged excitations of the mean orbital elements. It is thus an obvious requirement of our theory that the revolution period T_{orb} will disappear from the final solution. But the averaging procedure is a somewhat delicate task. It would be a mistake to average directly the instantaneous perturbations over both the rotational and the orbital timescales, because by doing so we would obtain the fast-rotation results depending on a single parameter σ_R , defined as $(\sigma_R/2\pi) \equiv \tau_R/T_{\text{orb}}$. A more careful treatment is needed so as the final results are defined on a larger domain, parametrized by the two quantities σ_R and r . Then, by taking the limit $r \rightarrow \infty$ we must recover the fast-rotation approximation.

The rest of this paper is organized as follows. In Section 2 we give a general scheme for the treatment of LAGEOS’s thermal response to external heating sources (Section 2.1), and compute the corresponding thermal force due to the solar radiation both with and without the eclipse effects arising when the orbit crosses the Earth’s shadow (Sections 2.2 and 2.3, respectively; some technical details of

the calculations have been moved to the Appendix). In Section 3 we apply this theory to the case of the LAGEOS satellite, and in particular we discuss how and when the generalized theory will modify the previous predictions on the long-term evolution of the orbital elements.

2. Theory

In the current context, we do not intend to follow Slabinski (1996) in taking into account the detailed structure of the LAGEOS satellite when modelling the heat transfer processes which result into the Yarkovsky-type thermal effects. We rather use a simple model close to that of Afonso *et al.* (1989) (see also Rubincam (1987) or Afonso *et al.* (1995)), namely a spherical satellite with radius R and homogeneous physical properties. Like in the fast-rotation case, this is likely to provide a fairly accurate model for the time dependence of the thermal effects, but subsequent empirical readjustments of the numerical parameters appearing in the final expressions will be required to obtain a good fit of the observed orbital residuals. Also, in computing the long-term dynamical effects, we are going to neglect the eccentricity of the orbit—a reasonable approximation, since its value for LAGEOS is $e \simeq 0.0044$.

2.1. Simple thermal model of LAGEOS

The basic assumptions of our approach are:

- we develop a linear theory in the temperature departure ΔT from its equilibrium value T_0 (i.e. terms of the order of $(\Delta T)^2$ are neglected);
- we use an energy balance equation at the satellite’s surface as an appropriate boundary condition for the heat transfer differential equation.

Thus, we assume that a “weak” external radiative energy flux $\Delta\Phi(t; R, \mathbf{n})$, impinging onto the outer satellite surface element of normal \mathbf{n} at the time t , causes a temperature perturbation $\Delta T(t; r, \mathbf{n})$ in the satellite body, i.e.

$$T(t; r, \mathbf{n}) = T_0 + \Delta T(t; r, \mathbf{n}). \quad (1)$$

The general heat transfer equation is

$$\kappa \nabla^2 [\Delta T(t; r, \mathbf{n})] = \rho C_p \frac{\partial \Delta T(t; r, \mathbf{n})}{\partial t} \quad (2)$$

(see, e.g. Landau and Lifschitz, 1986). Here κ is the thermal conductivity, ρ the density and C_p the specific heat. This equation links the divergence of the heat vector \mathbf{q} defined as

$$\mathbf{q} = -\kappa \nabla [\Delta T(t; r, \mathbf{n})] \quad (3)$$

to the time changes of the temperature field ΔT .

In our case the boundary condition just expresses the fact that energy is not piling up at the surface of the satellite, where as much energy is carried away by conduction and re-emitted radiation as is being brought in by the solar flux. This energy budget condition takes the following form:

$$\left[\kappa \frac{\partial \Delta T(t; r, \mathbf{n})}{\partial r} \right]_R + 4\varepsilon\sigma T_0^3 \Delta T(t; R, \mathbf{n}) = \alpha \Delta \Phi(t; R, \mathbf{n}) \quad (4)$$

where ε is the surface's thermal emissivity, α its absorption coefficient and σ the Stefan–Boltzmann constant.

The system of equations (2) and (4) represents a fairly complicated mathematical problem and different approximation methods can be envisaged for its solution. One possibility, not yet employed in the treatment of satellite thermal problems, would be to rewrite the Fourier equation (2) with the boundary condition (4) directly into the form of an equation for the surface temperature $\Delta T(t; R, \mathbf{n})$, looking for a proper junction of the solution at the centre of the satellite. The latter must satisfy a system of Volterra integral equations of the second kind, as shown by Landau and Lifschitz (1986) in the case of a one-dimensional problem. This rigorous method, however, is quite complex and lies beyond the scope of this paper.

In the following, we shall adopt a more direct approximate method, introduced by Rubincam (1987). It provides a fairly simple, analytical solution of the satellite thermal problem and, very important in this context, also allows one to carry out the next step—the computation of orbital perturbations—analytically. Actually, this method leads to an exponential factor expressing the “thermal memory” of the body (see equation (7)), which corresponds to the temporal part of the eigenfunctions constituting the Green's function of the diffusion problem (Morse and Feshbach, 1953).

A suitable tool for solving the parabolic diffusion equation (2) is the use of the Fourier transform (see Rubincam, 1987). By labelling the Fourier-transformed quantities with a superscript F, the solution for the temperature change ΔT related to the variable heating flux $\Delta \Phi$ is approximately

$$\Delta T^F(\nu) \simeq \frac{3\alpha}{\rho C_p R} \Delta \Phi^F(\nu) \frac{1}{\nu_R + i\nu} \quad (5)$$

(here i means the complex unit) with

$$\nu_R \equiv \frac{1}{\tau_R} \simeq \frac{12\varepsilon\sigma T_0^3}{\rho C_p R} \quad (6)$$

The exact numerical coefficients in these formulae are not essential because of our simplifying homogeneity assumption and the poor knowledge of the LAGEOS “mean” material constants. The fundamental property of solution (5) is its functional dependence upon frequency.

The computation of the inverse Fourier transform of solution (5) leads to

$$\Delta T(t; R, \mathbf{n}) = \frac{3\alpha}{\rho C_p R} \int_{t' < t} dt' \Delta \Phi(t'; R, \mathbf{n}') e^{-\nu_R(t-t')} \quad (7)$$

with the exponential damping kernel mentioned above. The effect of the satellite's rotation is hidden by the fact that in the integrand of equation (7) one must consider surface elements \mathbf{n}' at the retarded times t' which eventually become identical with the surface element \mathbf{n} at time t , appearing in the left-hand side of this equation. In our case, the uniform rotational motion is to be expressed by equation (11) below.

Once the temperature field $\Delta T(t; R, \mathbf{n})$ on the satellite

surface is known, the recoil force (per unit mass) \mathbf{a} caused by the emitted thermal radiation can be derived. If an isotropic (“Lambertian”) emission law is assumed, one gets

$$\mathbf{a}(t) = -\frac{8}{3} \frac{\varepsilon\sigma}{mc} T_0^3 \int dA(\theta, \phi) \Delta T[t; R, \mathbf{n}(\theta, \phi)] \mathbf{n}(\theta, \phi) \quad (8)$$

where the surface element is $dA(\theta, \phi) = R^2 \sin \theta d\theta d\phi$ (for the definition of the spherical angles θ and ϕ see Section 2.2 and Fig. 1). The integral on the right-hand side of equation (8) has to be performed over the whole satellite surface.

An alternative way to compute \mathbf{a} is by interchanging the two successive integrations in equations (7) and (8). We thus obtain

$$\mathbf{a}(t) = -\frac{8}{mc} \frac{\alpha\varepsilon\sigma}{\rho C_p R} T_0^3 \int_{t' < t} dt' e^{-\nu_R(t-t')} \mathbf{h}(t, t'; R) \quad (9)$$

where the “kernel function” $\mathbf{h}(t, t'; R)$ is defined by

$$\mathbf{h}(t, t'; R) = \int_{\Omega_*(t)} dA(\theta, \phi) \Delta \Phi(t'; R, \mathbf{n}') \mathbf{n}(\theta, \phi). \quad (10)$$

The integration domain $\Omega_*(t)$ in the previous integral is implicitly defined by the illumination condition $\Delta \Phi(t; R, \mathbf{n}) \geq 0$. It can be easily expressed explicitly in the coordinates (θ, ϕ) . Note that the integration on the right-hand side of equation (10) is performed over the domain $\Omega_*(t)$ given at the time t , whereas the flux projection $\Delta \Phi(t'; R, \mathbf{n}')$ in the integrand is taken at the retarded time t' .

We stress the different interpretations which can be made for the approaches based on equations (7) and (8) and equations (9) and (10), respectively, to compute the thermal force. In the former case, which more closely corresponds to intuition, one first establishes at a given time t the temperature field on the satellite surface (equation (7)) and then considers the contribution of all surface elements to the resulting thermal force (equation (8)). In the latter case, one starts by computing the first multiple moment of the illumination function $\Delta \Phi(t'; R, \mathbf{n}')$ (with the need to distinguish the time t and the retarded instant t' ; equation (9)) and then take into account the thermal relaxation processes characterized by an exponential damping (equation (10)). The second method is found to be much more suitable for the computation of the thermal force in the general non-stationary case (Section 2.3).

2.2. Yarkovsky–Schach effect, with no eclipses

We now introduce the following local reference frame: (i) the unit vector \mathbf{e}_z , characterizing the direction of the z -axis, along the instantaneous direction of the satellite's spin axis (\mathbf{s}), (ii) the unit vector \mathbf{e}_x , characterizing the direction of the x -axis, chosen in such a way that the x - z plane contains the instantaneous direction towards the Sun (\mathbf{n}_s). We then define a system of spherical coordinates (θ, ϕ) , attached to this reference frame in the usual manner.

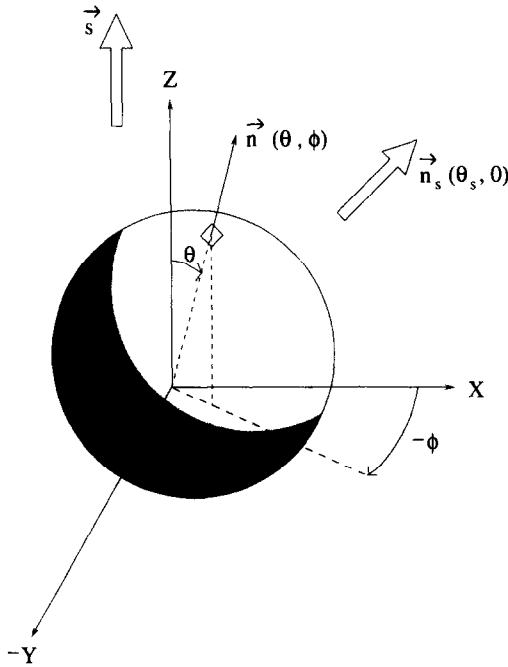


Fig. 1. Reference frame and geometrical quantities introduced in the text, \mathbf{s} is the satellite's spin vector, \mathbf{n}_s gives the direction of the Sun and \mathbf{n} is the normal to a satellite surface element

We thus have for instance $\mathbf{n}_s \equiv (\sin \theta_s, 0, \cos \theta_s)^T$. Figure 1 shows the geometrical quantities introduced above.

To define uniquely our problem we have still to specify two properties: (i) the rotation law of the satellite, and (ii) the external radiation flux. Consider a particular surface element $dA(\theta_0, \phi_0)$, parametrized by its position (θ_0, ϕ_0) at an arbitrary initial time t_0 . Then the rotation of the satellite is expressed by the position of this element at any time t :

$$\phi(t) = 2\pi\nu_r t + \phi_0, \theta = \theta_0. \quad (11)$$

Here, $\nu_r \equiv 1/T_{rot}$ is the rotational frequency of the satellite. As for the surface illumination, we assume a homogeneous radiation field with intensity I_0 , specified by the solar direction \mathbf{n}_s . Then the scalar radiation flux through the surface element characterized by a normal vector $\mathbf{n}(\theta, \phi)$ is given by

$$\Delta\Phi(R, \mathbf{n}) = I_0[\sin \theta_s \sin \theta \cos \phi + \cos \theta_s \cos \theta]. \quad (12)$$

By definition $\Delta\Phi$ must be positive for an illuminated surface element, otherwise its value is zero. From the physical point of view, I_0 is the "effective value" of the solar constant, including its annual variations due to the Earth's orbital eccentricity. Note that on the timescales $(T_{rot}, T_{orb}, \tau_R)$ relevant for our problem, the radiation flux $\Delta\Phi$ does not depend explicitly on the time t , that is we can neglect the much slower, "adiabatic" changes (in the sense of "adiabatic invariants") of the spin axis direction and the position of the Sun. This fact provides an important simplification of the problem in the case when the orbit undergoes no eclipse.

An important implication of the possibility of separating slowly and rapidly variable processes is that, within our model, the orbital timescale is totally absent in the physical description of the satellite thermal processes. It is thus natural to relate all the time periods to the basic timescale given by the satellite's rotation, T_{rot} . As a result,

for the purposes of this section we can define the auxiliary quantities $(\sigma'_R/2\pi) \equiv (\tau_R/T_{rot})$ and $\bar{e}' \equiv \exp(-2\pi/\sigma'_R)$, different from σ_R as defined in Section 1. Changing the integration variable in equation (7) using equation (11), we obtain for the temperature field ΔT

$$\Delta T(R, \mathbf{n}) = \frac{3\alpha}{2\pi\nu_r \rho C_p R} (1 - \bar{e}')^{-1} \times \int_{\phi-2\pi}^{\phi} d\phi' \Delta\Phi(R, \mathbf{n}') e^{-\sigma'_R(\phi - \phi')} \quad (13)$$

where $(1 - \bar{e}')^{-1}$ is obtained as the sum of an infinite geometric series, which accounts for the finite interval over which the following integral has to be calculated here. This integral can be computed easily for any surface element \mathbf{n} (we do not give here the corresponding lengthy but straightforward formulae). Equation (8) then yields the components of the thermal force per unit mass as

$$a_z = \gamma \cos \theta_s \quad (14)$$

$$a_x = \gamma \frac{\sin \theta_s}{1 + \sigma'_R{}^2} \quad (15)$$

$$a_y = \gamma \frac{\sin \theta_s \sigma'_R}{1 + \sigma'_R{}^2} \quad (16)$$

with the normalizing factor γ given by

$$\gamma = -\frac{16 \pi R^2 I_0}{3 mc} \tau_R T_0^3 \frac{\alpha \varepsilon \sigma}{\rho C_p R} \quad (17)$$

The spin-directed component a_z coincides with the usual fast-rotation expression (Afonso *et al.*, 1989; Farinella *et al.*, 1990), while the equatorial components vanish in the same approximation ($\sigma'_R \rightarrow \infty$). However, as soon as the LAGEOS rotation is slow enough, i.e. $T_{rot} \simeq \tau_R$, the latter components will no longer be negligible. Their perturbing effects will be discussed in Section 3.

The perturbing acceleration \mathbf{a} from equations (14) to (16) does not contribute to the averaged along-track force because it does not depend on the satellite's position along the orbit, hence it does not affect the semimajor axis evolution (since we are neglecting the eccentricity terms). However, it does contribute to the eccentricity/perigee excitation. Denoting Δh the real part and Δk the imaginary part of the excitation (i.e. $h = e \cos \omega$ and $k = e \sin \omega$, ω being the argument of perigee; see Tapley *et al.*, 1993; Métris *et al.*, 1996) we have

$$\Delta h = \frac{3}{2na} (\mathbf{a} \cdot \hat{\mathbf{b}}) + O(e) \quad (18)$$

$$\Delta k = -\frac{3}{2na} (\mathbf{a} \cdot \hat{\mathbf{a}}) + O(e) \quad (19)$$

where $n \equiv (2\pi/T_{orb})$ is the mean motion and a the semimajor axis of the orbit. The two unit vectors in the previous equations are defined as follows: $\hat{\mathbf{a}}$ is along the direction of the ascending node, $\hat{\mathbf{b}}$ lies in the orbital plane and $(\hat{\mathbf{a}}, \hat{\mathbf{b}})$ together with the orbital angular momentum vector form a direct triad of vectors.

2.3. *Yarkovsky–Schach effect, including eclipses*

Contrary to the previous case, the problem with the satellite’s orbit crossing the Earth’s shadow is no longer stationary, because the radiation flux $\Delta\Phi$ in equation (12) depends *explicitly* on time due to the interruption of the heating flux which occurs during eclipses. As a consequence, the thermal force is no longer constant along one satellite revolution around the Earth, and semimajor axis perturbations arise. To better explain our method of derivation in this case, we start with the special situation of a $N:1$ spin-orbit resonance, i.e. with the ratio r between the orbital and rotational periods coinciding with an integer number N . We stress that this assumption has no specific dynamical meaning here, but it is just a convenient “trick” to simplify the mathematical derivation. At the end of this section and in more detail in the Appendix, we will describe how the results can be generalized to any real value of the parameter r .

As mentioned in Section 2.1, the approach based on equations (9) and (10) for calculating the thermal force is more suitable in the non-stationary, shadow-crossing case. We thus start with the computation of the auxiliary vector quantity $\mathbf{h}(t, t')$ (the first moment of the insolation $\Delta\Phi$). Moreover, instead of time we shall use as a variable the satellite longitude along the orbit λ , measured from the ascending node and given by $\lambda = nt + \lambda_0$. With the resonance trick described above, we have

$$\phi(\lambda') = \phi(\lambda) + N(\lambda' - \lambda) \tag{20}$$

to be used in equation (10). Straightforward algebra leads to

$$\mathbf{h}(t, t'; R) = \frac{2\pi}{3} R^2 I_0 \begin{pmatrix} \sin \theta_s \cos N(\lambda - \lambda') \\ \sin \theta_s \sin N(\lambda - \lambda') \\ \cos \theta_s \end{pmatrix}. \tag{21}$$

Carrying out the remaining integration (9) is rather lengthy but not complicated, and leads to the following result for the three components of the thermal force per unit mass (in the same coordinate system we introduced in Section 2.2)

$$a_z = \gamma \cos \theta_s \psi_z(\lambda) \tag{22}$$

$$a_x = \gamma \frac{\sin \theta_s}{1 + N^2 \sigma_R^2} \psi_x(\lambda; N) \tag{23}$$

$$a_y = \gamma \frac{\sin \theta_s}{1 + N^2 \sigma_R^2} \psi_y(\lambda; N). \tag{24}$$

Note that now the thermal force depends explicitly on the satellite’s orbital longitude through the “shadow factors” $\psi(\lambda)$, which can be expressed as follows

$$\psi_z(\lambda) = \psi_{\text{shad}}(\lambda) + (1 - \bar{e})^{-1} (e^{\Delta_1/\sigma_R} - e^{\Delta_2/\sigma_R}) \tag{25}$$

$$\begin{aligned} \psi_x(\lambda; N) = & \psi_{\text{shad}}(\lambda) \\ & + (1 - \bar{e})^{-1} [e^{\Delta_1/\sigma_R} (\cos N\Delta_1 + N\sigma_R \sin N\Delta_1) \\ & - e^{\Delta_2/\sigma_R} (\cos N\Delta_2 + N\sigma_R \sin N\Delta_2)] \end{aligned} \tag{26}$$

$$\begin{aligned} \psi_y(\lambda; N) = & N\sigma_R \psi_{\text{shad}}(\lambda) \\ & + (1 - \bar{e})^{-1} [e^{\Delta_2/\sigma_R} (\sin N\Delta_2 - N\sigma_R \cos N\Delta_2) \\ & - e^{\Delta_1/\sigma_R} (\sin N\Delta_1 - N\sigma_R \cos N\Delta_1)]. \end{aligned} \tag{27}$$

Here $\psi_{\text{shad}}(\lambda)$ denotes the usual shadow function, equal to 0 when the satellite is inside the geometric shadow and 1 out of it, $\bar{e} \equiv \exp(-2\pi/\sigma_R)$ as before and the quantities Δ_1 and Δ_2 are given by

$$\Delta_1 = \begin{cases} \lambda_1 - \lambda, & \text{for } \lambda_1 < \lambda \\ \lambda_1 - \lambda - 2\pi, & \text{for } \lambda_1 > \lambda \end{cases} \tag{28}$$

and similarly for the index 2, with λ_1 and λ_2 denoting the orbital longitudes corresponding to entry into and exit from the Earth’s shadow, respectively. We observe that the polar force component a_z again coincides with that obtained using the fast-rotation assumption (see, i.e. Afonso *et al.*, 1989; Métris *et al.*, 1996). The equatorial components a_x and a_y average out in the fast-rotation case ($N \rightarrow \infty$), as expected owing to the absence of longitudinal (“diurnal”) temperature gradients.

Neglecting the eccentricity terms, the averaged along-track component of the perturbing acceleration $\mathbf{a}(\lambda)$ is given by

$$T = \frac{1}{2\pi} \int_0^{2\pi} d\lambda [-\sin \lambda \hat{\mathbf{a}} + \cos \lambda \hat{\mathbf{b}}] \cdot \mathbf{a}(\lambda) + O(e) \tag{29}$$

(Milani *et al.*, 1987), with the pair of unit vectors $(\hat{\mathbf{a}}, \hat{\mathbf{b}})$ defined as above.

We can also compute separately the along-track acceleration terms related to the three components of the thermal force (equations (22)–(24)). For this purpose, we define the following auxiliary projection parameters ($i = 1, 2$)

$$A_i^X = s_a^X \cos \lambda_i + s_b^X \sin \lambda_i \tag{30}$$

$$B_i^X = -s_a^X \sin \lambda_i + s_b^X \cos \lambda_i \tag{31}$$

where $s_a^X \equiv \mathbf{e}_X \cdot \hat{\mathbf{a}}$ and $s_b^X \equiv \mathbf{e}_X \cdot \hat{\mathbf{b}}$ are the projections of the base vector \mathbf{e}_X onto the pair of vectors $(\hat{\mathbf{a}}, \hat{\mathbf{b}})$. Analogous parameters can be introduced for the base vectors \mathbf{e}_Y and \mathbf{e}_Z . In the last case, we have $\mathbf{e}_Z = \mathbf{s}$, so that the A and B parameters correspond to the similar ones introduced by Scharroo *et al.* (1991) and Métris *et al.* (1996).

Using equations (22), (25) and (29) we obtain

$$T_z = \frac{\gamma}{2\pi} \frac{\sigma_R \cos \theta_s}{1 + \sigma_R^2} [A_1^Z - A_2^Z + \sigma_R (B_1^Z - B_2^Z)] \tag{32}$$

for the mean drag-like acceleration related to the spin-oriented thermal force component. Note that this result (i) does not depend on the parameter N , and (ii) coincides with the fast-rotation expression (see Scharroo *et al.*, 1991).

In a similar way, the equatorial force components yield the following averaged along-track perturbing accelerations:

$$\begin{aligned} T_x = & \frac{\gamma}{2\pi} \frac{\sin \theta_s}{[1 + (N-1)^2 \sigma_R^2][1 + (N+1)^2 \sigma_R^2]} \{ [1 + (N^2 + 1)\sigma_R^2] \\ & \times (A_1^X - A_2^X) + \sigma_R [1 - (N^2 - 1)\sigma_R^2] (B_1^X - B_2^X) \} \end{aligned} \tag{33}$$

$$T_Y = \frac{\gamma}{2\pi} \frac{N\sigma_R \sin \theta_s}{[1 + (N-1)^2\sigma_R^2][1 + (N+1)^2\sigma_R^2]} \times \{[1 + (N^2-1)\sigma_R^2](A_1^Y - A_2^Y) + 2\sigma_R(B_1^Y - B_2^Y)\}. \quad (34)$$

Both the components T_X and T_Y vanish in the fast-rotation approximation $N \rightarrow \infty$, as expected. Note, however, that the former component is characterized by a much faster decay with rotational frequency ($T_X \propto (1/N^2)$) than the latter one ($T_Y \propto (1/N)$). Therefore, the semimajor axis perturbation due to the T_Y component is more important for the LAGEOS case. We shall comment in more detail on the orbital effects associated with T_X and T_Y in Section 3.

We do not give here the laborious results for the eccentricity excitations in the eclipse case. However, we have verified that in analogy with the fast-rotation case (see Métris *et al.*, 1996), the contribution of the extra terms due to the eclipses are negligible with respect to the contribution of the basic terms (equations (18) and (19)).

In the rest of this section, we shall comment on the generalization of the previous results for any value of the ratio r between the revolution period T_{orb} and the rotation period T_{rot} . The difficulty is only of a technical character, and is related to the infinite domain of integration on the right-hand side of equation (9). The simplest way to deal with this problem is that of determining a suitable timescale for the periodicity of the vector \mathbf{h} . In the case of the exact $N:1$ resonance discussed above, we may take one revolution period as the natural ‘‘averaging scale’’, and summing up the geometrical series due to the presence of the exponential factor in the integrand we obtain

$$\mathbf{a}(\lambda) = -\frac{4}{\pi mc} \frac{\alpha \varepsilon \sigma T_0^3}{\rho C_p R} (1 - \bar{e})^{-1} \int_{\lambda - 2\pi}^{\lambda} d\lambda' \times e^{-\sigma_R(\lambda - \lambda')} \mathbf{h}(\lambda, \lambda'; R) \quad (35)$$

(we have again used the satellite’s orbital longitude λ instead of the time t as the independent variable). Alternatively, we can assume a rational representation of the parameter r , i.e. $r \equiv N/M$. Because the rational numbers are dense in the set of real numbers, by continuity our results will hold also for the general situation of any real value of r . Because the auxiliary vector $\mathbf{h}(t, t')$ from equation (10) takes now the form

$$\mathbf{h}(t, t'; R) = \frac{2\pi}{3} R^2 I_0 \begin{pmatrix} \sin \theta_s \cos r(\lambda - \lambda') \\ \sin \theta_s \sin r(\lambda - \lambda') \\ \cos \theta_s \end{pmatrix} \quad (36)$$

we realize that in this case the suitable timescale for its periodicity is $M \times T_{orb}$, rather than T_{orb} itself. Thus we modify the previous equation (35) into

$$\mathbf{a}(\lambda) = -\frac{4}{\pi mc} \frac{\alpha \varepsilon \sigma T_0^3}{\rho C_p R} (1 - \bar{e}^M)^{-1} \int_{\lambda - 2\pi M}^{\lambda} d\lambda' \times e^{-\sigma_R(\lambda - \lambda')} \mathbf{h}(\lambda, \lambda'; R). \quad (37)$$

Then we must take the time span $M \times T_{orb}$ as the average interval for the along-track perturbing acceleration. Clearly, the method is applicable if the final averaged result depends on the parameter r only, and not on the individual values of N and M . Lengthy calculations con-

firm this property and show that the final result is identical with that given in equations (32)–(34), provided the integer number N is substituted by the ratio r (see the Appendix for technical details). Note that formally this procedure is not justified when M is too large, as $M \times T_{orb}$ may become comparable to the timescales over which the orbital plane and the spin axis evolve; but in practice this cannot change the above conclusion if the latter timescales are long enough.

Of some interest might be also the long-term excitation of the mean orbital inclination I (see Farinella *et al.*, 1990; Tapley *et al.*, 1993). We shall not repeat the details of the computation procedure, which is the same as sketched above, and give only the final results, separately for the inclination excitations due to the three components of the thermal force. The spin-oriented force component yields

$$\left(\frac{dI}{dt}\right)_Z = \frac{\gamma}{\pi na} \frac{\cos \theta_s}{1 + \sigma_R^2} (\mathbf{s} \cdot \hat{\mathbf{e}}) \sin\left(\frac{\Delta_{sh}}{2}\right) (\cos \lambda_s - \sigma_R \sin \lambda_s). \quad (38)$$

Here, $\lambda_s \equiv (\lambda_1 + \lambda_2)/2 - \pi$ is the solar longitude measured along the satellite orbit from its node and $\Delta_{sh} \equiv (\lambda_2 - \lambda_1)/2$ the angular width of the Earth’s shadow measured in the orbital plane. This result is identical with that given by Farinella *et al.* (1990), an obvious consequence of the fact that this force component exactly coincides with the result of the fast-rotation approximation for the thermal effects. As for the contributions of the equatorial thermal force components, they are

$$\left(\frac{dI}{dt}\right)_X = \frac{\gamma}{\pi na} \frac{(\mathbf{e}_X \cdot \hat{\mathbf{e}}) \sin \theta_s}{[1 + (r-1)^2\sigma_R^2][1 + (r+1)^2\sigma_R^2]} \sin\left(\frac{\Delta_{sh}}{2}\right) \times \{[1 + (r^2+1)\sigma_R^2] \cos \lambda_s - \sigma_R [1 - (r^2-1)\sigma_R^2] \sin \lambda_s\} \quad (39)$$

$$\left(\frac{dI}{dt}\right)_Y = \frac{\gamma}{\pi na} \frac{(\mathbf{e}_Y \cdot \hat{\mathbf{e}}) r \sigma_R \sin \theta_s}{[1 + (r-1)^2\sigma_R^2][1 + (r+1)^2\sigma_R^2]} \sin\left(\frac{\Delta_{sh}}{2}\right) \times \{[1 + (r^2-1)\sigma_R^2] \cos \lambda_s - 2\sigma_R \sin \lambda_s\}. \quad (40)$$

3. Application to LAGEOS perturbations

In the framework of LAGEOS orbital studies, thermal effects have been discussed for the first time by Rubincam (1982). In that paper, Rubincam correctly identified the thermal effects due to the Earth’s IR radiation as a potentially important perturbation mechanism, although he did not give any detailed treatment for them. He also reported a suggestion of M. Schach that solar heating combined with eclipse passages may result in a net perturbing along-track force, and gave a qualitative description of this effect. Interestingly, this phenomenon had been already discussed and measured by Boudon *et al.* (1979), in the framework of the French accelerometric mission CAC-TUS.

In this paper, we limit our discussion to the orbital effects related to the interruption of the solar heating during the eclipse passages, i.e. to the Yarkovsky–Schach effect. From a physical point of view, the effect is due to the simple fact that the satellite cools down after it enters the Earth shadow, causing a change of the thermal force,

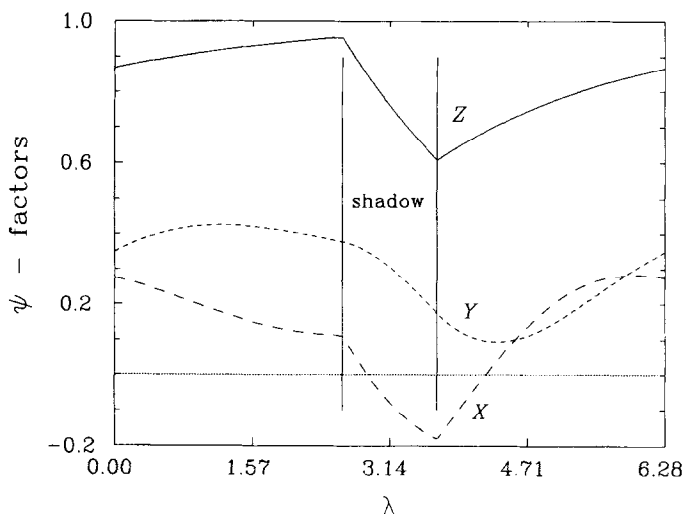


Fig. 2. Shadow factors $\psi(\lambda)$ appearing in the three components of the thermal force, plotted over one satellite revolution around the Earth. We have assumed a rotational period equal to the orbital one. The $\psi_Z(\lambda)$ factor appearing in the polar component is shown by the solid curve, whereas the dashed and dash-dotted curves represent the $\psi_X(\lambda)/(1 + \sigma_R^2)$ and the $\sigma_R \psi_Y(\lambda)/(1 + \sigma_R^2)$ factors appearing in the equatorial components, respectively. The Earth's shadow is assumed to be centred at $\lambda = \pi$, and the thermal lag parameter σ_R has been set to 2.4 rad

and heats up again after the satellite exits the shadow. In other words, following Rubincam (1982) we may say that the finite thermal lag corresponds to a “rotated position” of the effective Earth shadow, implying that the along-track component of the thermal force does not average out over one revolution. In our formulation, the cooling and heating of the satellite due to the shadow passages results in the presence of the “shadow factors” $\psi(\lambda)$ given by equations (25)–(27) in equations (22)–(24) for the instantaneous thermal force.

In Fig. 2 we plot these factors for $r = 1$, i.e. the exact spin-orbit resonance, and for a thermal lag parameter $\sigma_R = 2.4$ rad, a value close to that of LAGEOS according to the analysis of Métris *et al.* (1996). We centred the shadow position at $\lambda = \pi$ with $\lambda_1 = 2.6$, which corresponds approximately to the maximum width of the shadow for LAGEOS's orbit. The solid curve for $\psi_Z(\lambda)$ can be compared with Fig. 5 in Afonso *et al.* (1989), while the shadow factors related to the two equatorial force components have never been derived before. Although qualitatively similar, the three shadow factors are different in the details.

Figure 3 shows the dependence of the $\psi_X(\lambda; N)$ function on the parameter N , i.e. on the number of spin cycles completed during one satellite revolution around the Earth. In Part (a) the thermal lag parameter σ_R has been set again at 2.4 rad, the value estimated for LAGEOS by Métris *et al.* (1996). Besides having a decreasing amplitude, for higher values of N the curves approach a periodic function, with only a temporary influence of the eclipse passage. These properties lead to a rapid decrease of the mean value for increasing spin rates, in agreement with the expectation that the equatorial contribution to mean along-track perturbation should average out during one revolution when the rotation is fast enough. The qualitative features shown by the plots can be easily understood

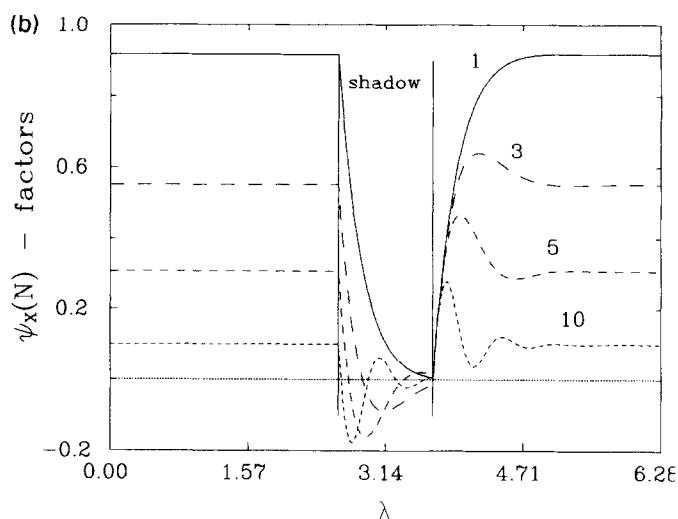
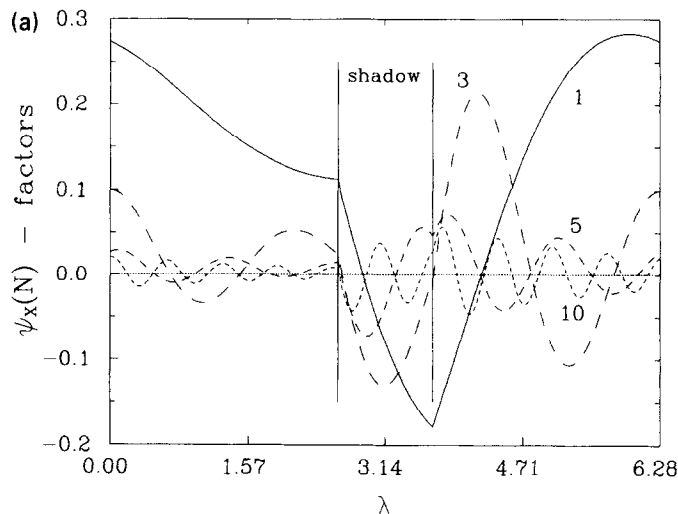


Fig. 3. The shadow factor $\psi_X(\lambda; N)/(1 + N^2 \sigma_R^2)$ associated with the X-component of the thermal force has been plotted vs. λ for different values of N , the ratio between the orbital and the rotational period: $N = 1$ (curve 1), 3 (curve 3), 5 (curve 5), and 10 (curve 10). The parameters in the upper part (a) of the figure are the same as in Fig. 2, whereas in part (b) we have taken $\sigma_R = 0.3$ rad

by considering that the force is approximately oriented towards the region on the satellite's surface with the lowest temperature, and that during a rotational cycle this region migrates on the satellite surface; at the same time, the eclipse entry/exit suddenly changes the intensity of the heating flux which causes a temperature gradient to arise on the surface. Because the large value of the thermal inertia parameter σ_R in part (a) of Fig. 3 partially hides this phenomenon, in part (b) we have plotted the same quantity but changed the value of σ_R to 0.3 rad. We observe that for a fast rotation (large N), the shadow passage excites a high-frequency and strongly damped wave pattern related to the satellite rotation. However, soon this pattern decays to the stationary value of the shadow factor, due to the low thermal lag parameter σ_R .

The Yarkovsky–Schach effect is well known to provide a significant contribution to the peaks/dips occurring in the sequence of observed LAGEOS semimajor axis residuals when the orbit crosses the Earth's shadow (Afonso *et al.*, 1989; Scharroo *et al.*, 1991; Farinella *et*

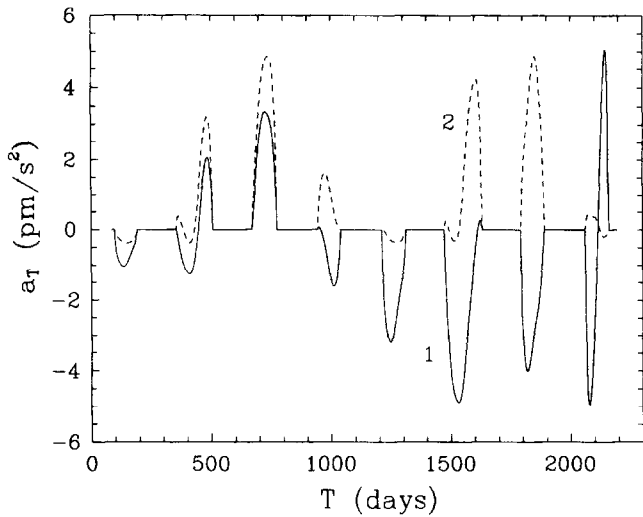


Fig. 4. Predictions of the averaged along-track acceleration on LAGEOS due to the Yarkovsky–Schach thermal effect vs. time (in days), starting on Jan. 1, 2005. The solid curve (1) has been derived from the generalized theory derived in this paper, including the effect of the equatorial thermal force components, while the dashed curve (2) corresponds to the usual fast-rotation approximation. Very large differences arise as the satellite’s spin rate slows down due to magnetic dissipation. At the end of the time span considered in this plot the 1:1 spin-orbit resonance is reached, and the Bertotti–less dynamical theory used to predict the evolution of LAGEOS’s rotational state ceases to be applicable. Following Métris *et al.* (1996), we have adopted the parameter values $\gamma = -175 \text{ pm s}^{-2}$ and $\sigma_R = 2.4 \text{ rad}$

al., 1996). Because here we are primarily interested in the future influence of the equatorial thermal force components, we have plotted in Fig. 4 the averaged along-track Yarkovsky–Schach perturbing acceleration starting from Jan. 1, 2005. Before this date the LAGEOS rotation is fast enough that only the polar force component (which remains unaltered in the fast-rotation case) plays a significant role.

The dashed curve in this figure shows the predictions obtained from the current fast-rotation case, which according to our results in about a decade will start to fail in a very substantial way (peaks instead of dips and vice versa).

After that, the generalized theory accounting for the equatorial thermal force components T_x and T_y will be an essential tool for LAGEOS orbital studies. Our simulation has been stopped after about 7 years, i.e. when the 1:1 spin-orbit resonance will be approached (i.e. $r \approx 1.1$), according to the Farinella *et al.* (1996) rotational evolution predictions. When this will happen, a more complex non-averaged theory will be needed to model the (possibly chaotic) subsequent spin evolution (Habib *et al.*, 1994). However, it is clear that the equatorial thermal force components will continue to play an important role in LAGEOS’s long-term orbital evolution.

Figure 5 shows our predictions for the eccentricity excitation effects due to the Yarkovsky–Schach effect. Métris *et al.* (1996) have recently shown that these effects account for a significant portion of the observed orbit residuals. It is thus important to understand whether the two additional force components will, in the future, sig-

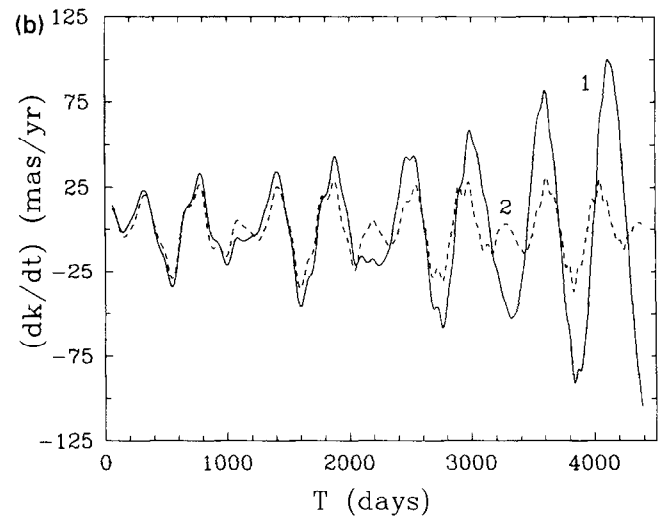
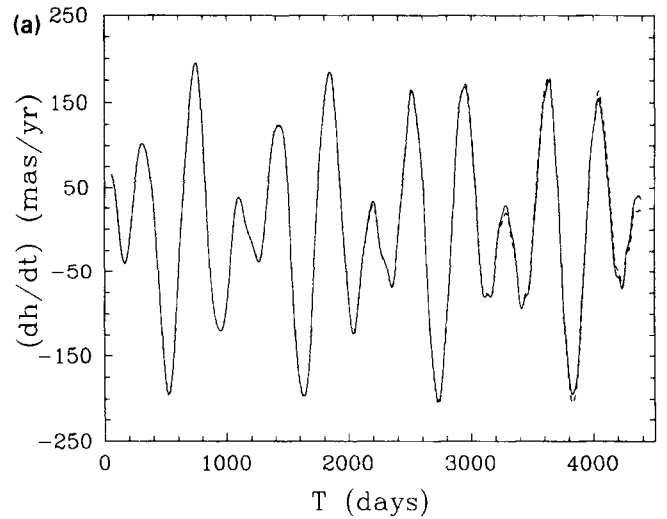


Fig. 5. Predictions on the excitation of LAGEOS’s orbital eccentricity vector due to the Yarkovsky–Schach thermal effect vs. time (in days), starting on Jan. 1, 1999. (a) Real component (\dot{h}) and (b) imaginary component (\dot{k}), both expressed in milli-arcseconds per year. The solid curves have been derived from the generalized theory derived in this paper, including the effect of the equatorial thermal force components, while the dashed curves correspond to the usual fast-rotation approximation. Note that the differences between the two sets of predictions are small for the real part but substantial for the imaginary part of the eccentricity excitation. The same parameter choice as in the previous semimajor axis predictions has been used here

nificantly modify the results obtained with the fast-rotation approximation.

The results shown in Fig. 5 suggest that there will be only a minor contribution of the equatorial thermal force components to the real eccentricity excitation component (which is affected in a dominant way by the spin-oriented force component), but that the opposite will hold for the imaginary component.

Finally, in Fig. 6 we have plotted the predicted inclination excitation due to the Yarkovsky–Schach effect, which was the subject of the Farinella *et al.* (1990) study in the fast-rotation approximation case. As before, that case (dashed curve, label 2) is now compared to the more general one with the equatorial components accounted for. We have used here two different parameter choices

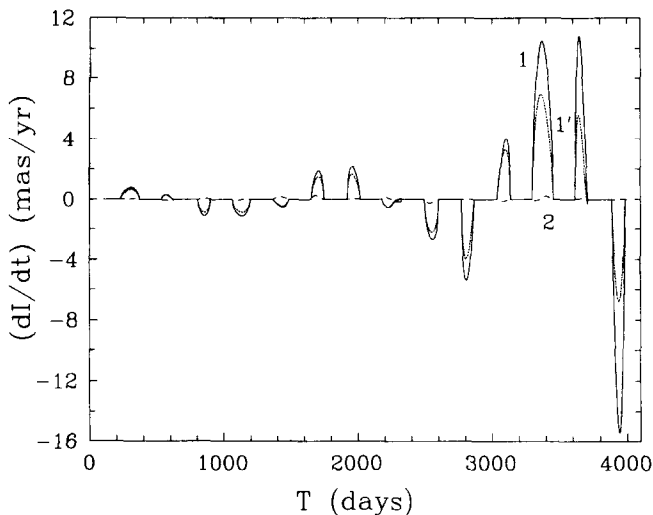


Fig. 6. Predictions of the averaged inclination excitation on LAGEOS due to the Yarkovsky–Schach thermal effect vs. time (in days), starting on Jan. 1, 2000. The solid curves (1 and 1') have been derived from the generalized theory derived in this paper, including the effect of the equatorial thermal force components, while the dashed curve (2) corresponds to the usual fast-rotation approximation. Again significant differences appear as the satellite rotation period approaches the 1:1 resonance with the revolution period (at the end of the plotted time span). The following parameter values have been used here: $\gamma = -175 \text{ pm s}^{-2}$, $\sigma_R = 2.4 \text{ rad}$ for curves 1 and 2 (in agreement with Métris *et al.* (1996)), and $\gamma = -82 \text{ pm s}^{-2}$, $\sigma_R = 1.45 \text{ rad}$ for curve 1' (following Scharroo *et al.* (1991)). Both these combinations match equally well the along-track residuals, but they show slightly different patterns in the inclination series

(corresponding to the solid curves 1 and 1'), to illustrate a point which may become important. Our results indicate that an analysis of the inclination effects in the future may allow us to decorrelate the two parameters appearing in the thermal force model, i.e. the normalizing factor γ and the phase lag σ_R . As we remarked in Section 1, the exact values of these parameters depend in a fairly sensitive way on the detailed thermal properties and structure of the satellite. As pointed out by Métris *et al.* (1996), the same purpose may be achieved by an analysis of the eccentricity excitation components. But other perturbing effects overlap the thermal ones in a different way for different orbital elements, so the inclination data will possibly supply important additional information.

4. Conclusions

The main results obtained in this paper can be summarized as follows:

1. We have developed a fairly general theory for the thermal effects on the dynamics of LAGEOS-type artificial satellites, avoiding the usual fast-rotation approximation and applicable for any ratio between the rotational, orbital and thermal relaxation timescales. In this paper we have studied in particular the Yarkovsky–Schach perturbation effects arising from the solar heating of the satellite and its interruptions by eclipses. The second paper of this series will deal with

the Yarkovsky–Rubincam effect caused by Earth IR radiation heating.

2. In the case of LAGEOS, a growing influence of the components of the thermal force not aligned with the spin axis is predicted in the near future, due to the rapid despin of the satellite by magnetic dissipation effects. Applying the theory developed here will be essential after about year 2005 to correctly model the Yarkovsky–Schach perturbations affecting the long-term semimajor axis decay of LAGEOS's orbit.
3. Important future discrepancies from the fast-rotation case are predicted also for the perturbations affecting the imaginary part of the eccentricity excitation and the inclination excitation of LAGEOS. These effects in some cases are sensitive to the individual values of two thermal parameters, which cannot be decorrelated from an analysis of the semimajor axis residuals only.

Acknowledgements. We are grateful to D. P. Rubincam, another anonymous referee and G. Métris for several constructive remarks. P.F. acknowledges partial support from the Italian Space Agency (ASI) and from the Italian Ministry for University and Scientific Research (MURST). D.V. is grateful to the University of Pisa (Italy) for its kind hospitality and to the Observatoire de la Côte d'Azur (Dept. CERGA, Grasse, France), where he could perform this work thanks to the "H. Poincaré" research fellowship.

References

- Afonso, G., Barlier, F. and Carpino, M., Orbital effects of LAGEOS seasons and eclipses. *Ann. Geophys.* **7**, 501–514, 1989.
- Afonso, G., Gomes, R. S. and Florczak, M. A., Asteroid fragments in Earth-crossing orbits. *Planet. Space Sci.* **43**, 787–795, 1995.
- Barlier, F., Carpino, M. and Farinella, P., Non-gravitational perturbations on the semimajor axis of LAGEOS. *Ann. Geophys.* **4A**, 193–210, 1986.
- Bertotti, B. and Iess, L., The rotation of LAGEOS. *J. Geophys. Res.* **96**, 2431–2440, 1991.
- Boudon, Y., Barlier, F. and Bernard, A., Synthesis of flight results of the Cactus accelerometer for accelerations below $10^{-9}g$. *Acta Astronautica* **6**, 1387–1398, 1979.
- Burns, J. A., Lamy, P. L. and Soter, S., Radiation forces on small particles in the Solar System. *Icarus* **40**, 1–48, 1979.
- Farinella, P., Nobili, A. M., Barlier, F. and Mignard, F., Effects of thermal thrust on the node and inclination of LAGEOS. *Astron. Astrophys.* **234**, 546–554, 1990.
- Farinella, P., Vokrouhlický, D. and Barlier, F., The rotation of LAGEOS and its long-term semimajor axis decay: a self-consistent solution. *J. Geophys. Res.* **101**, 17,861–17,872, 1996.
- Habib, S., Holz, D. E. and Kheifetz, A., Spin dynamics of the LAGEOS satellite in support of a measurement of the Earth's gravitomagnetism. *Phys. Rev.* **D50**, 6068–6079, 1994.
- Landau, L. D. and Lifschitz, E. M., *Hydrodynamics*. Nauka, Moscow, 1986 (in Russian).
- Métris, G. and Vokrouhlický, D., Thermal force perturbations of the LAGEOS orbit: the albedo radiation part. *Planet. Space Sci.* **44**, 611–617, 1996.
- Métris, G., Vokrouhlický, D., Ries, J. C. and Eanes, R. J., Non-gravitational phenomena and the LAGEOS eccentricity excitations. *J. Geophys. Res.* 1996 (submitted).

- Milani, A., Nobili, A. M. and Farinella, P.**, *Non-gravitational Perturbations and Satellite Geodesy*. A. Hilger, Bristol, 1987.
- Morse, P. M. and Feshbach, H.**, *Methods of Theoretical Physics*. McGraw-Hill, New York, 1953.
- Peterson, C.**, A source mechanism for meteorites controlled by the Yarkovsky effect. *Icarus* **29**, 91–111, 1976.
- Ries, J. C., Eanes, R. J. and Watkins, M. M.**, Spin vector influence on LAGEOS ephemeris, presented at the Second Meeting of IAG Special Study Group 2.130, Baltimore, 1993.
- Robbins, J. W., Williamson, R. G. and Rubincam, D. P.**, LAGEOS I and II spin axis evolution. *EOS Trans. AGU* **75**, 109–110, 1994.
- Rubincam, D. P.**, On the secular decrease in the semimajor axis of LAGEOS's orbit. *Celest. Mech.* **26**, 361–382, 1982.
- Rubincam, D. P.**, LAGEOS orbit decay due to infrared radiation from Earth. *J. Geophys. Res.* **92**, 1287–1294, 1987.
- Rubincam, D. P.**, Yarkovsky thermal drag on LAGEOS. *J. Geophys. Res.* **93**, 13805–13810, 1988.
- Rubincam, D. P.**, Drag on the LAGEOS satellite. *J. Geophys. Res.* **95**, 4881–4886, 1990.
- Scharroo, R., Wakker, K. F., Ambrosius, B. A. C. and Noomen, R.**, On the along-track acceleration of the LAGEOS satellite. *J. Geophys. Res.* **96**, 729–740, 1991.
- Slabinski, V. J.**, LAGEOS acceleration due to intermittent solar heating during eclipses periods. *Bull. Am. Astron. Soc.* **20**, 902, 1988.
- Slabinski, V. J.**, A numerical solution for LAGEOS thermal thrust: the rapid-spin case. *Celest. Mech.* 1996 (in press).
- Tapley, B. D., Schutz, B. E., Eanes, R. J., Ries, J. C. and Watkins, M. M.**, LAGEOS laser ranging contributions to geodynamics, geodesy, and orbital dynamics, in *Contributions of Space Geodesy to Geodynamics: Earth Dynamics* (edited by D. E. Smith and D. L. Turcotte), pp. 147–173. AGU, Washington, DC, 1993.

Appendix

As announced in Section 2.3, this appendix is devoted to some technical details of the averaging method used to derive the long-term along-track force. The method itself is outlined in Section 2.3, and is based on taking a rational approximation for the r parameter: $r \equiv N/M$, with N and M integer numbers. Since the component of the perturbing acceleration directed along the spin axis does not depend on N and/or r , we will limit our discussion here to the other two components.

First, we define the auxiliary functions

$$\hat{C}(r, \bar{e}) = \frac{1 - \bar{e} \cos(2\pi r)}{1 - 2\bar{e} \cos(2\pi r) + \bar{e}^2} \quad (\text{A1})$$

$$\hat{S}(r, \bar{e}) = \frac{\bar{e} \sin(2\pi r)}{1 - 2\bar{e} \cos(2\pi r) + \bar{e}^2}. \quad (\text{A2})$$

Then, we proceed to perform the double integration, over the averaging timescale and the thermal relaxation timescale, to obtain the long-term perturbing acceleration. We treat separately the two equatorial components of the thermal force. After several rearrangements of the integrals, they can be reduced to

$$T_X = \frac{\gamma}{2\pi} \frac{\sin \theta_s}{1 + r^2 \sigma_R^2} \int_0^{2\pi} d\lambda [-\sin \lambda \hat{\mathbf{a}} + \cos \lambda \hat{\mathbf{b}}] \cdot \mathbf{e}_X \times [\hat{C}(r, \bar{e}) \psi_C(\lambda) - \hat{S}(r, \bar{e}) \psi_S(\lambda)] \quad (\text{A3})$$

$$T_Y = \frac{\gamma}{2\pi} \frac{\sin \theta_s}{1 + r^2 \sigma_R^2} \int_0^{2\pi} d\lambda [-\sin \lambda \hat{\mathbf{a}} + \cos \lambda \hat{\mathbf{b}}] \cdot \mathbf{e}_Y \times [\hat{C}(r, \bar{e}) \psi_S(\lambda) + \hat{S}(r, \bar{e}) \psi_C(\lambda)]. \quad (\text{A4})$$

Here the γ coefficient is the same as in equation (17), and the shadow factors ψ_C and ψ_S are defined as

$$\psi_C(\lambda) = \{1 - \bar{e}[\cos(2\pi r) - r\sigma_R \sin(2\pi r)]\} \psi_{\text{shad}}(\lambda) + e^{\Delta_1/\sigma_R} [\xi_1^-(\lambda; r, \sigma_R) \cos r\Delta_1 + \xi_1^+(\lambda; r, \sigma_R) \sin r\Delta_1] - e^{\Delta_2/\sigma_R} [\xi_2^-(\lambda; r, \sigma_R) \cos r\Delta_2 + \xi_2^+(\lambda; r, \sigma_R) \sin r\Delta_2] \quad (\text{A5})$$

$$\psi_S(\lambda) = \{r\sigma_R - \bar{e}[\sin(2\pi r) + r\sigma_R \cos(2\pi r)]\} \psi_{\text{shad}}(\lambda) - e^{\Delta_1/\sigma_R} [\xi_1^-(\lambda; r, \sigma_R) \sin r\Delta_1 - \xi_1^+(\lambda; r, \sigma_R) \cos r\Delta_1] + e^{\Delta_2/\sigma_R} [\xi_2^-(\lambda; r, \sigma_R) \sin r\Delta_2 - \xi_2^+(\lambda; r, \sigma_R) \cos r\Delta_2]. \quad (\text{A6})$$

We also introduced

$$\xi_i^-(\lambda; r, \sigma_R) = \begin{cases} \cos(2\pi r) - r\sigma_R \sin(2\pi r), & \text{for } \lambda_i > \lambda \\ 1, & \text{for } \lambda_i < \lambda \end{cases} \quad (\text{A7})$$

and

$$\xi_i^+(\lambda; r, \sigma_R) = \begin{cases} \sin(2\pi r) + r\sigma_R \cos(2\pi r), & \text{for } \lambda_i > \lambda \\ r\sigma_R, & \text{for } \lambda_i < \lambda \end{cases}. \quad (\text{A8})$$

For integer values of the parameter r the previous results can be simplified into those given in equations (32)–(34). A straightforward integration of equations (A3) and (A4) yields

$$T_X = \frac{\gamma}{2\pi} \frac{\sin \theta_s}{[1 + (r-1)^2 \sigma_R^2][1 + (r+1)^2 \sigma_R^2]} \times \{[1 + (r^2 + 1)\sigma_R^2](A_1^X - A_2^X) + \sigma_R[1 - (r^2 - 1)\sigma_R^2](B_1^X - B_2^X)\} \quad (\text{A9})$$

$$T_Y = \frac{\gamma}{2\pi} \frac{r\sigma_R \sin \theta_s}{[1 + (r-1)^2 \sigma_R^2][1 + (r+1)^2 \sigma_R^2]} \times \{[1 + (r^2 - 1)\sigma_R^2](A_1^Y - A_2^Y) + 2\sigma_R(B_1^Y - B_2^Y)\} \quad (\text{A10})$$

as given in Section 2.3 and used in the subsequent analysis of the LAGEOS orbital effects.